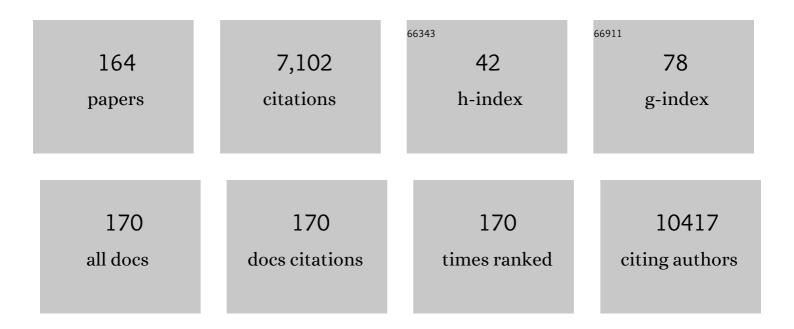
List of Publications by Year in descending order

Source: https://exaly.com/author-pdf/2027677/publications.pdf Version: 2024-02-01



#	Article	IF	CITATIONS
1	Asymmetric cell design for decoupled hydrogen and oxygen evolution paired with V(II)/V(III) redox mediator. Catalysis Today, 2022, 403, 67-73.	4.4	3
2	Harvesting Low-Grade Waste Heat to Electrical Power Using a Thermoelectrochemical Cell Based on a Titanium Carbide Electrode. ACS Applied Energy Materials, 2022, 5, 2130-2137.	5.1	8
3	Liquefied-Natural-Gas-Derived Vertical Carbon Layer Deposited on SiO as Cost-Effective Anode for Li-Ion Batteries. Journal of the Electrochemical Society, 2022, 169, 020528.	2.9	9
4	Low-hysteresis manganese hexacyanoferrate (MnHCF) aqueous battery for low-grade thermal energy harvesting. Journal of Power Sources, 2022, 524, 231080.	7.8	3
5	Promoting Oxygen Evolution Reaction Induced by Synergetic Geometric and Electronic Effects of IrCo Thin-Film Electrocatalysts. ACS Catalysis, 2022, 12, 6334-6344.	11.2	12
6	Effects of Variation of Heat Flux Released from the Meniscus on the Surface Shape of the Solidified Shell During Continuous Casting. Metals and Materials International, 2021, 27, 5346-5359.	3.4	1
7	Tailoring Binding Abilities by Incorporating Oxophilic Transition Metals on 3D Nanostructured Ni Arrays for Accelerated Alkaline Hydrogen Evolution Reaction. Journal of the American Chemical Society, 2021, 143, 1399-1408.	13.7	161
8	Trace amounts of Ru-doped Ni–Fe oxide bone-like structures <i>via</i> single-step anodization: a flexible and bifunctional electrode for efficient overall water splitting. Journal of Materials Chemistry A, 2021, 9, 12041-12050.	10.3	30
9	Three-Dimensionally Interconnected Nanoporous IrRe Thin Films Prepared by Selective Etching of Re for Oxygen Evolution Reaction. ACS Applied Energy Materials, 2021, 4, 4173-4180.	5.1	8
10	Electrochemical synthesis of zinc ricinoleate and its application in ammonia adsorption. Journal of Environmental Chemical Engineering, 2021, 9, 105083.	6.7	0
11	10 μ4m-thick MoO3-coated TiO2 nanotubes as a volume expansion regulated binder-free anode for lithium ion batteries. Journal of Industrial and Engineering Chemistry, 2021, 96, 364-370.	5.8	10
12	Cost-efficient nickel-based thermo-electrochemical cells for utilizing low-grade thermal energy. Journal of Power Sources, 2021, 494, 229705.	7.8	23
13	Ni _{0.67} Fe _{0.33} Hydroxide Incorporated with Oxalate for Highly Efficient Oxygen Evolution Reaction. ACS Applied Materials & Interfaces, 2021, 13, 42870-42879.	8.0	30
14	Hybrid thermo-electrochemical energy harvesters for conversion of low-grade thermal energy into electricity via tungsten electrodes. Applied Energy, 2021, 299, 117334.	10.1	16
15	Oxygen reduction reaction of vertically-aligned nanoporous Ag nanowires. Applied Catalysis B: Environmental, 2021, 298, 120586.	20.2	20
16	Visualization of Transition Metal Decoration on h-BN Surface. Nano Letters, 2021, 21, 10562-10569.	9.1	5
17	Comparision of Antioxidant and Physiological Activities of Processed Waters Generated during Red Bean Paste Preparation. Journal of the Korean Society of Food Science and Nutrition, 2021, 50, 1168-1176.	0.9	1
18	Phase-tuned nanoporous vanadium pentoxide as binder-free cathode for lithium ion battery.	5.2	17

² Electrochimica Acta, 2020, 330, 135192.

#	Article	IF	CITATIONS
19	Inâ€Situ Precipitationâ€Induced Growth of Leafâ€like CuO Nanostructures on Cu–Ni Alloys for Binderâ€Free Anodes in Liâ€lon Batteries. ChemSusChem, 2020, 13, 419-425.	6.8	13
20	Reuse of wastewater discharged from thermal-plasma decomposition of chlorodifluoromethane: Production of titanium dioxide nanopowder. Journal of Cleaner Production, 2020, 250, 119542.	9.3	4
21	Enhanced Activity and Stability of Nanoporous Ptlr Electrocatalysts for Unitized Regenerative Fuel Cell. ACS Applied Energy Materials, 2020, 3, 1423-1428.	5.1	9
22	Enhancing Electrochemical CO ₂ Reduction Activity <i>via</i> Charge Transfer and sp-Band Filling in a Au Thin Layer on Ag. ACS Applied Energy Materials, 2020, 3, 9792-9798.	5.1	5
23	A General Strategy to Atomically Dispersed Precious Metal Catalysts for Unravelling Their Catalytic Trends for Oxygen Reduction Reaction. ACS Nano, 2020, 14, 1990-2001.	14.6	116
24	Self-activated anodic nanoporous stainless steel electrocatalysts with high durability for the hydrogen evolution reaction. Electrochimica Acta, 2020, 364, 137315.	5.2	26
25	Extremely fast electrochromic supercapacitors based on mesoporous WO3 prepared by an evaporation-induced self-assembly. NPG Asia Materials, 2020, 12, .	7.9	76
26	Alginic Acid from Padina boryana Abate Particulate Matter-Induced Inflammatory Responses in Keratinocytes and Dermal Fibroblasts. Molecules, 2020, 25, 5746.	3.8	8
27	Ag layer deposited on Zn by physical vapor deposition with enhanced CO selectivity for electrochemical CO2 reduction. Applied Surface Science, 2020, 526, 146651.	6.1	26
28	Cu-Based Thermoelectrochemical Cells for Direct Conversion of Low-Grade Waste Heat into Electricity. ACS Applied Energy Materials, 2020, 3, 6383-6390.	5.1	26
29	Controlled contribution of Ni and Cr cations to stainless steel 304 electrode: Effect of electrochemical oxidation on electrocatalytic properties. Electrochemistry Communications, 2020, 117, 106770.	4.7	10
30	Selective electrocatalysis imparted by metal–insulator transition for durability enhancement of automotive fuel cells. Nature Catalysis, 2020, 3, 639-648.	34.4	79
31	Highly active coral-like porous silver for electrochemical reduction of CO2 to CO. Journal of CO2 Utilization, 2020, 41, 101242.	6.8	16
32	Electrocatalyst design for promoting two-electron oxygen reduction reaction: Isolation of active site atoms. Current Opinion in Electrochemistry, 2020, 21, 109-116.	4.8	39
33	Inverseâ€direction Growth of TiO ₂ Microcones by Subsequent Anodization in HClO ₄ for Increased Performance of Lithiumâ€lon Batteries. ChemElectroChem, 2020, 7, 1248-1255.	3.4	3
34	Atomically dispersed Pt–N4 sites as efficient and selective electrocatalysts for the chlorine evolution reaction. Nature Communications, 2020, 11, 412.	12.8	154
35	Microwave-assisted evolution of WO ₃ and WS ₂ /WO ₃ hierarchical nanotrees. Journal of Materials Chemistry A, 2020, 8, 9654-9660.	10.3	18
36	Effects of the Ultrasound Treatment on Reaction Rates in the RH Processor Water Model System. Metals and Materials International, 2019, 25, 238-247.	3.4	3

#	Article	IF	CITATIONS
37	Tempcore Process Simulator to Analyze Microstructural Evolution of Quenched and Tempered Rebar. Applied Sciences (Switzerland), 2019, 9, 2938.	2.5	10
38	A double raster laser scanning strategy for rapid die-less bending of 3D shape. Journal of Materials Research and Technology, 2019, 8, 4741-4756.	5.8	15
39	Enhanced rate capability due to highly active Ta2O5 catalysts for lithium sulfur batteries. Journal of Power Sources, 2019, 435, 226707.	7.8	21
40	Polyethylenimineâ€assisted Synthesis of Au Nanoparticles for Efficient Syngas Production. Electroanalysis, 2019, 31, 1401-1408.	2.9	12
41	Simulation Perspectives of Sub-1V Single-Supply Z ² -FET 1T-DRAM Cells for Low-Power. IEEE Access, 2019, 7, 40279-40284.	4.2	8
42	Critical role of elemental copper for enhancing conversion kinetics of sulphur cathodes in rechargeable magnesium batteries. Applied Surface Science, 2019, 484, 933-940.	6.1	22
43	Anion additives in rapid breakdown anodization for nonmetal-doped TiO2 nanotube powders. Electrochemistry Communications, 2019, 109, 106610.	4.7	12
44	Steam reforming of methanol for ultra-pure H2 production in a membrane reactor: Techno-economic analysis. International Journal of Hydrogen Energy, 2019, 44, 2330-2339.	7.1	38
45	CO2 reforming of methane for H2 production in a membrane reactor as CO2 utilization: Computational fluid dynamics studies with a reactor geometry. International Journal of Hydrogen Energy, 2019, 44, 2298-2311.	7.1	27
46	Enhanced Activity for Oxygen Evolution Reaction of Nanoporous IrNi thin film Formed by Electrochemical Selective Etching Process. Journal of Electrochemical Science and Technology, 2019, 10, 402-407.	2.2	9
47	Cellular properties of the fermented microalgae PavlovaÃ⁻¿¼lutheri and its isolated active peptide in osteoblastic differentiation of MG‑63 cells. Molecular Medicine Reports, 2018, 17, 2044-2050.	2.4	8
48	Tungsten Carbide as a Highly Efficient Catalyst for Polysulfide Fragmentations in Li–S Batteries. Journal of Physical Chemistry C, 2018, 122, 7664-7669.	3.1	39
49	Current Collapse-Free and Self-Heating Performances in Normally Off GaN Nanowire GAA-MOSFETs. IEEE Journal of the Electron Devices Society, 2018, 6, 354-359.	2.1	5
50	Electrochemically Activated Iridium Oxide Black as Promising Electrocatalyst Having High Activity and Stability for Oxygen Evolution Reaction. ACS Energy Letters, 2018, 3, 1110-1115.	17.4	48
51	Improved performance of dual-conducting polymer-coated sulfur composite with high sulfur utilization for lithium-sulfur batteries. Journal of Alloys and Compounds, 2018, 742, 868-876.	5.5	29
52	Polyselenide Anchoring Using Transition-Metal Disulfides for Enhanced Lithium–Selenium Batteries. Inorganic Chemistry, 2018, 57, 2149-2156.	4.0	19
53	Protective effect of polysaccharides from Celluclast-assisted extract of Hizikia fusiforme against hydrogen peroxide-induced oxidative stress in vitro in Vero cells and in vivo in zebrafish. International Journal of Biological Macromolecules, 2018, 112, 483-489.	7.5	77
54	Performance enhancement of molten carbonate-based direct carbon fuel cell (MC-DCFC) via adding mixed ionic-electronic conductors into Ni anode catalyst layer. Journal of Power Sources, 2018, 386, 28-33.	7.8	16

#	Article	IF	CITATIONS
55	Soft-template synthesis of mesoporous non-precious metal catalyst with Fe-N x /C active sites for oxygen reduction reaction in fuel cells. Applied Catalysis B: Environmental, 2018, 222, 191-199.	20.2	115
56	Catalyst-Doped Anodic TiO2 Nanotubes: Binder-Free Electrodes for (Photo)Electrochemical Reactions. Catalysts, 2018, 8, 555.	3.5	30
57	Purification and Identification of an Antioxidative Peptide from Digestive Enzyme Hydrolysis of Cutlassfish Muscle. Journal of Aquatic Food Product Technology, 2018, 27, 934-944.	1.4	6
58	Morphology Dependence on Surface-Enhanced Raman Scattering Using Gold Nanorod Arrays Consisting of Agglomerated Nanoparticles. Plasmonics, 2017, 12, 203-208.	3.4	15
59	Heterogeneous Catalysis for Lithium–Sulfur Batteries: Enhanced Rate Performance by Promoting Polysulfide Fragmentations. ACS Energy Letters, 2017, 2, 327-333.	17.4	174
60	An upper limit of Cr-doping level to Retain Zero-strain Characteristics of Li4Ti5O12 Anode Material for Li-ion Batteries. Scientific Reports, 2017, 7, 43335.	3.3	29
61	CO ₂ Electroreduction on Au/TiC: Enhanced Activity Due to Metal–Support Interaction. ACS Catalysis, 2017, 7, 2101-2106.	11.2	69
62	Enhanced performance of sulfur-infiltrated bimodal mesoporous carbon foam by chemical solution deposition as cathode materials for lithium sulfur batteries. Scientific Reports, 2017, 7, 42238.	3.3	20
63	Highly active and selective Au thin layer on Cu polycrystalline surface prepared by galvanic displacement for the electrochemical reduction of CO2 to CO. Applied Catalysis B: Environmental, 2017, 213, 211-215.	20.2	53
64	Au coated PS nanopillars as a highly ordered and reproducible SERS substrate. Photonics and Nanostructures - Fundamentals and Applications, 2017, 25, 65-71.	2.0	14
65	High density Ag nanobranches decorated with sputtered Au nanoparticles for surface-enhanced Raman spectroscopy. Applied Surface Science, 2017, 410, 525-529.	6.1	19
66	Hydrogen Oxidationâ€Selective Electrocatalysis by Fine Tuning of Pt Ensemble Sites to Enhance the Durability of Automotive Fuel Cells. ChemSusChem, 2017, 10, 489-493.	6.8	24
67	Extended Analysis of the \$Z^{2}\$ -FET: Operation as Capacitorless eDRAM. IEEE Transactions on Electron Devices, 2017, 64, 4486-4491.	3.0	34
68	Platinum Single Atoms on Carbon Nanotubes as Efficient Catalyst for Hydroalkoxylation. Bulletin of the Korean Chemical Society, 2017, 38, 1221-1225.	1.9	5
69	Shape-Controlled Synthesis of Dumbbell-like Pt–Fe ₃ O ₄ –MnO <i>_x</i> Nanoparticles by Governing the Reaction Kinetics. ACS Omega, 2017, 2, 8483-8489.	3.5	9
70	Balancing activity, stability and conductivity of nanoporous core-shell iridium/iridium oxide oxygen evolution catalysts. Nature Communications, 2017, 8, 1449.	12.8	250
71	Shape and Composition Control of Monodisperse Hybrid Pt-CoO Nanocrystals by Controlling the Reaction Kinetics with Additives. Scientific Reports, 2017, 7, 3851.	3.3	16
72	Platinum single atoms dispersed on carbon nanotubes as reusable catalyst for Suzuki coupling reaction. Journal of Catalysis, 2017, 352, 388-393.	6.2	46

#	Article	IF	CITATIONS
73	\${Z}^{extsf {2}}\$ -FET as Capacitor-Less eDRAM Cell For High-Density Integration. IEEE Transactions on Electron Devices, 2017, 64, 4904-4909.	3.0	28
74	Pd–Sn Alloy Electrocatalysts for Interconversion Between Carbon Dioxide and Formate/Formic Acid. Journal of Nanoscience and Nanotechnology, 2017, 17, 7547-7555.	0.9	13
75	Fabrication of normally-off GaN nanowire gate-all-around FET with top-down approach. Applied Physics Letters, 2016, 109, .	3.3	23
76	Effects of transition metal doping in Pt/M-TiO2 (MÂ=ÂV, Cr, and Nb) on oxygen reduction reaction activity. Journal of Power Sources, 2016, 320, 188-195.	7.8	65
77	Bifunctional Interface of Au and Cu for Improved CO ₂ Electroreduction. ACS Applied Materials & Interfaces, 2016, 8, 23022-23027.	8.0	93
78	Direct access to aggregation-free and small intermetallic nanoparticles in ordered, large-pore mesoporous carbon for an electrocatalyst. RSC Advances, 2016, 6, 88255-88264.	3.6	12
79	Protective effects of polysaccharides from Psidium guajava leaves against oxidative stresses. International Journal of Biological Macromolecules, 2016, 91, 804-811.	7.5	43
80	On the mechanism of high product selectivity for HCOOH using Pb in CO ₂ electroreduction. Physical Chemistry Chemical Physics, 2016, 18, 9652-9657.	2.8	60
81	Shaped Ir–Ni bimetallic nanoparticles for minimizing Ir utilization in oxygen evolution reaction. Chemical Communications, 2016, 52, 5641-5644.	4.1	78
82	Gallic Acid-g-Chitosan Modulates Inflammatory Responses in LPS-Stimulated RAW264.7 Cells Via NF-κB, AP-1, and MAPK Pathways. Inflammation, 2016, 39, 366-374.	3.8	73
83	Electrochemical Properties of Lithium Sulfur Battery with Silicon Anodes Lithiated by Direct Contact Method. Journal of Electrochemical Science and Technology, 2016, 7, 228-233.	2.2	7
84	Electrochemical Properties of Lithium Sulfur Battery with Silicon Anodes Lithiated by Direct Contact Method. Journal of Electrochemical Science and Technology, 2016, 7, 228-233.	2.2	3
85	Bifunctional enhancement of oxygen reduction reaction activity on Ag catalysts due to water activation on LaMnO3 supports in alkaline media. Scientific Reports, 2015, 5, 13552.	3.3	47
86	Effect of a Surface Area and a d-Band Oxidation State on the Activity and Stability of RuOxElectrocatalysts for Oxygen Evolution Reaction. Bulletin of the Korean Chemical Society, 2015, 36, 1874-1877.	1.9	4
87	Enhanced Oxygen Reduction Reaction Activity Due to Electronic Effects between Ag and Mn ₃ O ₄ in Alkaline Media. ACS Catalysis, 2015, 5, 3995-4002.	11.2	115
88	Protective effect of carvacrol from Thymus quinquecostatus Celak against tert-butyl hydroperoxide-induced oxidative damage in Chang cells. Food Science and Biotechnology, 2015, 24, 735-741.	2.6	3
89	Analysis of the origin of periodic oscillatory flow in the continuous casting mold. Metals and Materials International, 2015, 21, 295-302.	3.4	7
90	A Mo-doped TiNb ₂ O ₇ anode for lithium-ion batteries with high rate capability due to charge redistribution. Chemical Communications, 2015, 51, 9849-9852.	4.1	125

#	Article	IF	CITATIONS
91	Electrochemical Characteristic Change of Cr-doped Li ₄ Ti ₅ O ₁₂ due to Different Water Solubility of Dopant Precursors. Journal of the Korean Electrochemical Society, 2015, 18, 17-23.	0.1	0
92	Enhancement of Activity and Durability through Cr Doping of TiO ₂ Supports in Pt Electrocatalysts for Oxygen Reduction Reactions. ChemCatChem, 2014, 6, 3239-3245.	3.7	11
93	Examination of chemical and physical effects on sump screen clogging of containment materials used in Korean plants. Annals of Nuclear Energy, 2014, 69, 51-56.	1.8	5
94	Anomalously increased oxygen reduction reaction activity with accelerated durability test cycles for platinum on thiolated carbon nanotubes. Chemical Communications, 2014, 50, 596-598.	4.1	16
95	Activity–Stability Trends for the Oxygen Evolution Reaction on Monometallic Oxides in Acidic Environments. Journal of Physical Chemistry Letters, 2014, 5, 2474-2478.	4.6	569
96	Using Surface Segregation To Design Stable Ruâ€ir Oxides for the Oxygen Evolution Reaction in Acidic Environments. Angewandte Chemie - International Edition, 2014, 53, 14016-14021.	13.8	331
97	Enhancing triple-phase boundary at fuel electrode of direct carbon fuel cell using a fuel-filled ceria-coated porous anode. International Journal of Hydrogen Energy, 2014, 39, 17314-17321.	7.1	21
98	Enhancing Ni anode performance via Gd 2 O 3 addition in molten carbonate-type direct carbon fuel cell. International Journal of Hydrogen Energy, 2014, 39, 16541-16547.	7.1	21
99	Compressive strain as the main origin of enhanced oxygen reduction reaction activity for Pt electrocatalysts on chromium-doped titania support. Applied Catalysis B: Environmental, 2014, 158-159, 112-118.	20.2	50
100	Flame aerosol synthesis of carbon-supported Pt–Ru catalysts for a fuel cell electrode. International Journal of Hydrogen Energy, 2014, 39, 14416-14420.	7.1	16
101	Stabilization of Oxygen-deficient Structure for Conducting Li4Ti5O12-δ by Molybdenum Doping in a Reducing Atmosphere. Scientific Reports, 2014, 4, 4350.	3.3	85
102	Fucoxanthin derivatives from Sargassum siliquastrum inhibit matrix metalloproteinases by suppressing NF-ήB and MAPKs in human fibrosarcoma cells. Algae, 2014, 29, 355-366.	2.3	15
103	Seahorse-derived peptide suppresses invasive migration of HT1080 fibrosarcoma cells by competing with intracellular I±-enolase for plasminogen binding and inhibiting uPA-mediated activation of plasminogen. BMB Reports, 2014, 47, 691-696.	2.4	6
104	The cycling performances of lithium–sulfur batteries in TEGDME/DOL containing LiNO3 additive. Ionics, 2013, 19, 1795-1802.	2.4	35
105	Enhanced corrosion resistance and fuel cell performance of Al1050 bipolar plate coated with TiN/Ti double layer. Energy Conversion and Management, 2013, 75, 727-733.	9.2	25
106	Controlled synthesis of La1â^'xSrxCrO3 nanoparticles by hydrothermal method with nonionic surfactant and their ORR activity in alkaline medium. Materials Research Bulletin, 2013, 48, 3651-3656.	5.2	13
107	Free standing acetylene black mesh to capture dissolved polysulfide in lithium sulfur batteries. Chemical Communications, 2013, 49, 11107.	4.1	74
108	Sputter-deposited ZnO thin films consisting of nano-networks for binder-free dye-sensitized solar cells. Current Applied Physics, 2013, 13, 381-385.	2.4	6

#	Article	IF	CITATIONS
109	Blockâ€Copolymerâ€Assisted Oneâ€Pot Synthesis of Ordered Mesoporous WO _{3â^`<i>x</i>/i>} /Carbon Nanocomposites as Highâ€Rateâ€Performance Electrodes for Pseudocapacitors. Advanced Functional Materials, 2013, 23, 3747-3754.	14.9	145
110	Purification of antioxidative peptide from peptic hydrolysates of Mideodeok (Styela clava) flesh tissue. Food Science and Biotechnology, 2013, 22, 541-547.	2.6	20
111	Strong Interaction between Pt and Thiolated Carbon for Electrocatalytic Durability Enhancement. ACS Catalysis, 2013, 3, 3067-3074.	11.2	34
112	Enhanced Gas Sensing Performance of Hydrophilic Graphite Nanoparticles Synthesized by Liquid Phase Pulsed Laser Ablation. Journal of Nanoscience and Nanotechnology, 2013, 13, 7020-7024.	0.9	1
113	Characteristic Corrosion Resistance of Nanocrystalline TiN Films Prepared by High Density Plasma Reactive Magnetron Sputtering. Journal of Nanoscience and Nanotechnology, 2013, 13, 4601-4607.	0.9	0
114	Evaluation of the formability of a bipolar plate manufactured from aluminum alloy Al 1050 using the rubber pad forming process. Proceedings of the Institution of Mechanical Engineers, Part B: Journal of Engineering Manufacture, 2012, 226, 909-918.	2.4	20
115	Anomalous decrease in structural disorder due to charge redistribution in Cr-doped Li4Ti5O12 negative-electrode materials for high-rate Li-ion batteries. Energy and Environmental Science, 2012, 5, 9903.	30.8	143
116	Codoping effect of Li1.1V0.9O2 anodes for lithium-ion batteries with Mo and W (Li1.1V0.9â^'2xMoxWxO2): Based on electronic structure calculations using full-potential KKR-Green's function method. Journal of Alloys and Compounds, 2012, 526, 135-138.	5.5	4
117	Fabrication of hierarchical ZnO nanostructures for dye-sensitized solar cells. Electrochimica Acta, 2012, 78, 417-421.	5.2	42
118	Bioactive Compounds Extracted from Ecklonia cava by Using Enzymatic Hydrolysis Protects High Glucose-Induced Damage in INS-1 Pancreatic β-Cells. Applied Biochemistry and Biotechnology, 2012, 167, 1973-1985.	2.9	17
119	Site-Specific Transition Metal Occupation in Multicomponent Pyrophosphate for Improved Electrochemical and Thermal Properties in Lithium Battery Cathodes: A Combined Experimental and Theoretical Study. Journal of the American Chemical Society, 2012, 134, 11740-11748.	13.7	37
120	Prevention of oxidative stress in Chang liver cells by gallic acid-grafted-chitosans. Carbohydrate Polymers, 2012, 87, 876-880.	10.2	26
121	Phase change of bimetallic PdCo electrocatalysts caused by different heat-treatment temperatures: Effect on oxygen reduction reaction activity. Journal of Catalysis, 2012, 290, 65-78.	6.2	28
122	Enhanced electrocatalytic performance due to anomalous compressive strain and superior electron retention properties of highly porous Pt nanoparticles. Journal of Catalysis, 2012, 291, 69-78.	6.2	29
123	Direct covalent thiolation of carbon nanotube supports to enhance the durability of highly loaded Pt electrocatalysts. Electrochemistry Communications, 2012, 19, 85-89.	4.7	5
124	Shuttle inhibitor effect of lithium perchlorate as an electrolyte salt for lithium–sulfur batteries. Journal of Applied Electrochemistry, 2012, 42, 75-79.	2.9	21
125	Electrochemical Properties of Li1.1V0.75W0.075Mo0.075O2/Graphite Composite Anodes for Lithium-ion Batteries. Bulletin of the Korean Chemical Society, 2012, 33, 65-68.	1.9	4
126	Effect of Al Content on the Gas-Phase Dehydration of Glycerol over Silica-Alumina-Supported Silicotungstic Acid Catalysts. Bulletin of the Korean Chemical Society, 2012, 33, 2369-2377.	1.9	7

#	Article	IF	CITATIONS
127	Hydrophilic Graphite Nanoparticles Synthesized by Liquid Phase Pulsed Laser Ablation and Their Carbon-composite Sensor Application. Journal of the Korean Electrochemical Society, 2012, 15, 236-241.	0.1	0
128	Ultrastable Aqueous Graphite Nanofluids Prepared by Single-step Liquid-phase Pulsed Laser Ablation (LP-PLA). Chemistry Letters, 2011, 40, 768-769.	1.3	7
129	Isolation and identification of an antioxidant flavonoid compound from citrus-processing by-product. Journal of the Science of Food and Agriculture, 2011, 91, 1925-1927.	3.5	42
130	Analyses on Fine Structure and Electronic Structure of Cr-doped Li4Ti5O12by Using X-ray Absorption Spectroscopy and First Principle Calculation. Journal of the Korean Electrochemical Society, 2011, 14, 33-37.	0.1	1
131	Electrochemical Immunosensor Using a Gas Diffusion Layer as an Immobilization Matrix. Bulletin of the Korean Chemical Society, 2011, 32, 1975-1979.	1.9	0
132	Surface Thiolation of MCMB to Support Sn Nanoparticles for Anode Materials of Lithium Ion Batteries. Chemistry Letters, 2010, 39, 610-611.	1.3	4
133	Additive treatment effect of TiO2 as supports for Pt-based electrocatalysts on oxygen reduction reaction activity. Electrochimica Acta, 2010, 55, 3628-3633.	5.2	81
134	Anticancer effect of lipids partially purified from Pacific oyster, Crassostrea gigas on PC3 cells. Food Science and Biotechnology, 2010, 19, 213-217.	2.6	8
135	Temperature dependence of morphology and oxygen reduction reaction activity for carbon-supported Pd–Co electrocatalysts. Journal of Applied Electrochemistry, 2010, 40, 1917-1923.	2.9	14
136	Facile and rapid synthesis of zinc oxalate nanowires and their decomposition into zinc oxide nanowires. Journal of Crystal Growth, 2010, 312, 2946-2951.	1.5	16
137	Platinum dendrites with controlled sizes for oxygen reduction reaction. Electrochemistry Communications, 2010, 12, 1596-1599.	4.7	49
138	Catalytic oxidation kinetics of iron-containing carbon particles generated by spraying ferrocene-mixed with diesel fuel into a hydrogen–air diffusion flame. Carbon, 2010, 48, 2072-2084.	10.3	21
139	Investigation of developed precipitates in AlMgSiCu alloys with and without excess Si. Materials Science and Technology, 2010, 26, 440-444.	1.6	10
140	PtRu nano-dandelions on thiolated carbon nanotubes: a new synthetic strategy for supported bimetallic core–shell clusters on the atomic scale. Chemical Communications, 2010, 46, 2085.	4.1	29
141	Gas-phase Dehydration of Glycerol over Supported Silicotungstic Acids Catalysts. Bulletin of the Korean Chemical Society, 2010, 31, 3283-3290.	1.9	24
142	Fine Structure Effect of PdCo electrocatalyst for Oxygen Reduction Reaction Activity: Based on X-ray Absorption Spectroscopy Studies with Synchrotron Beam. Journal of Electrochemical Science and Technology, 2010, 1, 31-38.	2.2	6
143	Roles of Surface Steps on Pt Nanoparticles in Electro-oxidation of Carbon Monoxide and Methanol. Journal of the American Chemical Society, 2009, 131, 15669-15677.	13.7	186
144	Thermo-Chemical Analysis of a Calcination Furnace to Produce Cathode Material for the Secondary Batteries. Journal of the Korean Electrochemical Society, 2009, 12, 155-161.	0.1	0

#	Article	IF	CITATIONS
145	Asymmetric dehydration of β-hydroxy esters and application to the syntheses of flavane derivatives. Tetrahedron, 2008, 64, 1515-1522.	1.9	19
146	Thermal Instability of Cycled Li _{<i>x</i>} Ni _{0.5} Mn _{0.5} O ₂ Electrodes: An in Situ Synchrotron X-ray Powder Diffraction Study. Chemistry of Materials, 2008, 20, 4936-4951.	6.7	87
147	Changes in the Crystal Structure and Electrochemical Properties of Li[sub x]Ni[sub 0.5]Mn[sub 0.5]O[sub 2] during Electrochemical Cycling to High Voltages. Journal of the Electrochemical Society, 2007, 154, A566.	2.9	46
148	Oxidation treatment of carbon nanotubes: An essential process in nanocomposite with RuO2 for supercapacitor electrode materials. Applied Physics Letters, 2006, 89, 033107.	3.3	22
149	Structural and electronic properties of Ptn (n = 3, 7, 13) clusters on metallic single wall carbon nanotube. Physica Status Solidi (B): Basic Research, 2006, 243, 3472-3475.	1.5	32
150	Electronic structures of Pt clusters adsorbed on (5,5) single wall carbon nanotube. Chemical Physics Letters, 2006, 432, 213-217.	2.6	71
151	Competitive effect of carbon nanotubes oxidation on aqueous EDLC performance: Balancing hydrophilicity and conductivity. Journal of Power Sources, 2006, 158, 1517-1522.	7.8	101
152	Surface thiolation of carbon nanotubes as supports: A promising route for the high dispersion of Pt nanoparticles for electrocatalysts. Journal of Catalysis, 2006, 238, 394-401.	6.2	166
153	Fine Size Control of Platinum on Carbon Nanotubes: From Single Atoms to Clusters. Angewandte Chemie - International Edition, 2006, 45, 407-411.	13.8	211
154	Formation of Single Pt Atoms on Thiolated Carbon Nanotubes Using a Moderate and Large-Scale Chemical Approach. Advanced Materials, 2006, 18, 2634-2638.	21.0	25
155	Highly dispersed ruthenium oxide nanoparticles on carboxylated carbon nanotubes for supercapacitor electrode materials. Journal of Materials Chemistry, 2005, 15, 4914.	6.7	157
156	Drastic change of electric double layer capacitance by surface functionalization of carbon nanotubes. Applied Physics Letters, 2005, 87, 234106.	3.3	88
157	Thermally Stable Gel Polymer Electrolytes. Journal of the Electrochemical Society, 2003, 150, A439.	2.9	41
158	Enzymic properties of recombinant BACE2. FEBS Journal, 2002, 269, 5668-5677.	0.2	12
159	Isolation and Characterization of Antioxidative Peptides from Gelatin Hydrolysate of Alaska Pollack Skin. Journal of Agricultural and Food Chemistry, 2001, 49, 1984-1989.	5.2	413
160	Thermal stability enhancement of Cu/WN/SiOF/Si multilayers by post-plasma treatment of fluorine-doped silicon dioxide. Journal of Applied Physics, 1999, 85, 473-477.	2.5	9
161	Leader Peptidase from Escherichia coli: Overexpression, Characterization, and Inactivation by Modification of Tryptophan Residues 300 and 310 with N-Bromosuccinimide1. Journal of Biochemistry, 1995, 117, 535-544.	1.7	18
162	Thermo-Chemical Analysis of a Calcination Furnace to Produce Cathode Material for the Secondary Batteries. Advanced Materials Research, 0, 413, 477-485.	0.3	0

#	Article	IF	CITATIONS
163	Combined Effect of Catholyte Gap and Cell Voltage on Syngas Ratio in Continuous CO ₂ /H ₂ O Co-electrolysis. Journal of Electrochemical Science and Technology, 0, , .	2.2	4
164	The influence of laser powder-bed fusion microstructures on the corrosion behavior of CuSn alloy. Journal of Materials Science, 0, , 1.	3.7	1